

## ***Ab initio* study of the valence-electron relaxation effect on x-ray-emission spectra and the excitonic effect on electron-energy-loss spectra of the Si $L_{2,3}$ edge**

H. Ma, S. H. Lin, R. W. Carpenter, and O. F. Sankey

Center for Solid State Science, Tempe, Arizona 85287-1704

(Received 1 April 1991)

The valence-band-electron relaxation effect on x-ray-emission spectra and the excitonic effect on electron-energy-loss spectra of the Si  $L_{2,3}$  edge were studied using an *ab initio* self-consistent pseudo-atomic-orbital method with large unit cells. Comparisons of our theoretical results with experimental x-ray-emission and electron-energy-loss spectra of the Si  $L_{2,3}$  edge suggest that there is very little relaxation of valence-band electrons before the  $2p$  core hole is filled by one of the valence electrons. When including the excitonic effect in electron-energy-loss near-edge-structure calculations, the valence band should therefore be kept the same as the ground state.

### I. INTRODUCTION

In the electron-energy-loss process of the Si  $L_{2,3}$  edge, one of the  $2p$  electrons is excited into the conduction band and leaves behind a core hole. During the excitation process the excited electron interacts with the core hole, and thus may have final states in the conduction band that are different from the ones calculated using the ground-state energy-band theory. This is the so-called "excitonic effect." Perturbation theories have been developed to include this effect in x-ray-absorption near-edge structures (XANES) and electron-energy-loss near-edge structures (EELNES).<sup>1-3</sup> The effective-mass theory for the weak Wannier exciton<sup>4</sup> was used to calculate the Si  $L_{2,3}$  near-edge structure, producing good agreement with experiment within 1 eV of the threshold.<sup>5</sup> The  $(Z+1)$  approximation has been combined with an impurity Green's-function method to calculate the core excitons in hexagonal BN by Robertson,<sup>6</sup> and in semiconductors by Hjalmanson, Buttner, and Dow.<sup>7</sup> Similar procedures have also been used by Mele and Ritsko<sup>8</sup> and by Disko *et al.*<sup>9</sup> Zunger<sup>10</sup> used a self-consistent one-electron model with broken symmetries to calculate core-ionization, core-exciton, and core-to-conduction-band transition energies for GaP. He showed that the screening of the core-hole self-energy by the electron orbit is important in explaining the experimentally determined core-exciton binding energies. In the present paper, we calculate the excitonic effect of the Si  $L_{2,3}$  edge by using an *ab initio* large-unit-cell approach, which includes the complete relaxation of valence-band electrons.

Similar to the excited electron in the conduction band, the electrons in the valence band can also feel the presence of the core hole through Coulomb interactions. The valence-band electrons may relax before the core hole is filled by a valence electron through Auger or x-ray-emission processes. These relaxation effects are in principle contained in the x-ray-emission spectra. A secondary aim of this work is to compare x-ray-emission spectra with the theoretical results of the ground state with no relaxation of valence electrons and the excited state with

complete relaxation of valence electrons. This comparison could reveal the extent of the relaxation of electrons in the valence band.

In the present work, the core-hole effect of the Si  $L_{2,3}$  edge was included self-consistently by using a large-unit-cell energy-band scheme. The energy-band program we used utilizes an *ab initio* self-consistent linear combination of pseudo-atomic-orbitals scheme.<sup>11</sup> The calculations were performed within the local-density approximation and used a linear combination of  $sp^3d^5$  pseudo-atomic-orbitals. This method was shown to yield nearly identical results with the rigorous plane-wave-basis expansion formulation,<sup>11</sup> but its results are more conveniently adapted to calculations of electron-energy-loss and x-ray-emission spectra.

The large-unit-cell procedure consists of two steps. The first step is to calculate the pseudopotential and pseudo-atomic-orbitals of the atoms by using an atomic calculation program.<sup>12</sup> The pseudopotentials and pseudo-atomic-orbitals of the excited Si atom, Si\*, are generated by promoting a  $2p$  core electron to the valence orbitals. For convenience this Si atom with a  $2p$  core hole will be denoted as Si\* in the remainder of this paper. In the second step, a large unit cell was constructed with the Si atom at the origin being replaced by the Si\* atom and the energy-band structure is computed self-consistently. The large unit cell is used to reduce the interaction between the Si\* atoms so that the calculation is close to an isolated Si\* atom. Again for convenience the energy-band structure calculated in this way is called the energy-band structure of the "excited state." The energy-band structures of crystalline Si were calculated for both the ground and excited states, and the results were used to compute the electron-energy-loss absorption and x-ray-emission spectra of the Si  $L_{2,3}$  edge. Our results are then compared with experimental data.

In Sec. II, we briefly describe the generation of the pseudopotential and pseudo-atomic-orbitals for the Si atom with a  $2p$  core hole and the calculation of the energy band and density of states using a large unit cell. The theory of electron-energy-loss cross sections will be

presented in Sec. III. Results and discussions will be given in Sec. IV and the conclusions in Sec. V.

## II. ENERGY-BAND CALCULATION

The Bloch basis function for wave vector  $\mathbf{k}$  and atomic orbital  $\mu$  is defined as

$$\Phi_{\mu}(\mathbf{k}, \mathbf{r}) = (1/\sqrt{N}) \sum_l e^{i\mathbf{k} \cdot (\mathbf{l} + \mathbf{b})} \phi_{\mu}^{\text{PAO}}(\mathbf{r} - \mathbf{l} - \mathbf{b}), \quad (1)$$

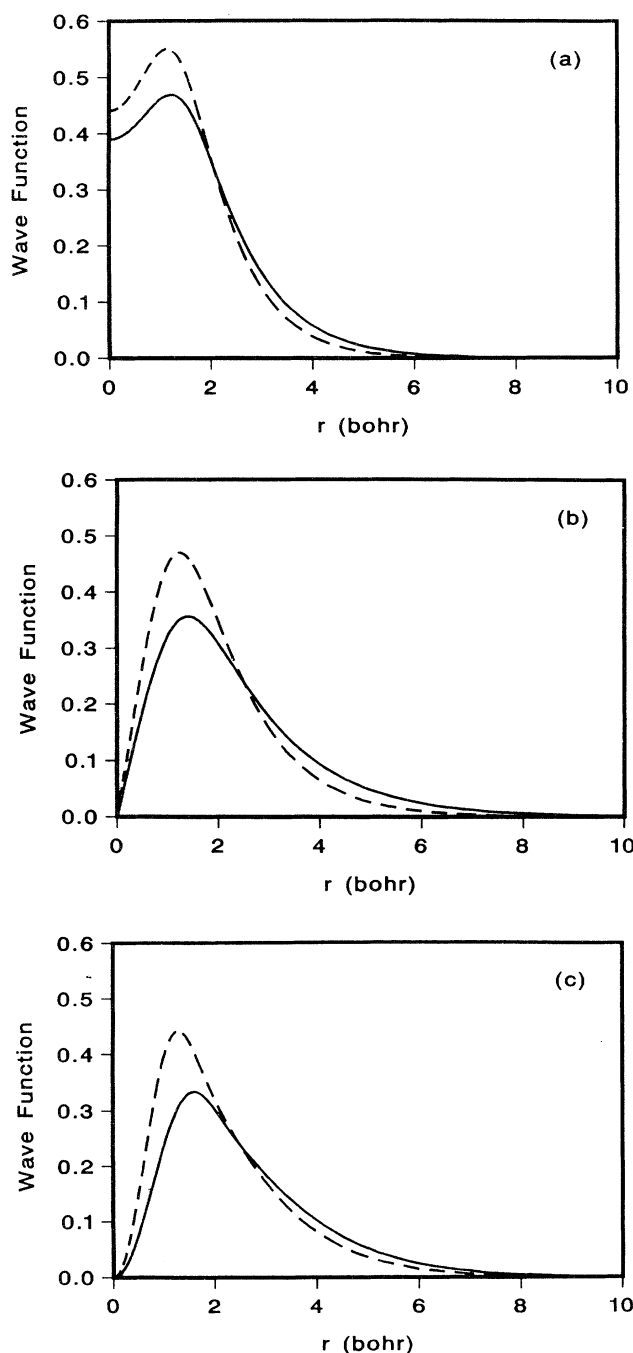


FIG. 1. Wave functions of pseudo-atomic-orbitals, (a)  $s$ , (b)  $p$ , and (c)  $d$ . The solid lines are those of Si and the dashed lines are those of Si\*.

where  $l$  sums over all the unit cells in the crystal and  $\mathbf{b}$  is the basis vector of the basis atom,  $\mu$ , within the unit cell. The pseudo-atomic-orbitals  $\phi_{\mu}^{\text{PAO}}(\mathbf{r})$  are the valence atomic orbitals of the isolated atom computed self-consistently using the same pseudopotential and local-density approximation (LDA) as the solid.<sup>11</sup> The PAO's are numerical solutions of the atomic system, which are fit to analytical forms for computational convenience. The radial part of the PAO is fit to a sum of Slater orbitals of the form

$$\phi_{\mu}^{\text{PAO}}(r) = \sum_{i=1}^3 (A_i + r A_{i+3} + r^2 A_{i+6}) e^{-\alpha_i r}. \quad (2)$$

The  $3s$  and  $3p$  PAO's of Si were generated using the ground-state configuration,  $1s^2 2s^2 2p^6 3s^2 3p^2$ . The  $3d$  PAO was derived using the excited-state configuration,  $1s^2 2s^2 2p^6 3s^1 3p^{0.75} 3d^{0.25}$ .<sup>12</sup> The  $3s$  and  $3p$  PAO's of Si\* were generated by promoting one electron from the  $2p$  level to the  $3d$  level, i.e., using the excited-state configuration,  $1s^2 2s^2 2p^5 3s^2 3p^2 3d^1$ . The  $3d$  PAO of Si\* was derived using the configuration  $1s^2 2s^2 2p^5 3s^1 3p^1 3d^1$ . The PAO's of Si\* are compared with those of Si in Fig. 1. Due to the extra Coulomb attraction of the core hole the PAO's of Si\* are more contracted toward the origin than those of Si. The fitted parameters of the PAO's of Si and Si\* are given in Table I.

The pseudopotentials we used are of the Hamann-Schluter-Chiang type<sup>13</sup> with the radial cutoffs determined

TABLE I. Pseudo-atomic-orbital parameters of Si and Si\* in atomic units.

$i$	1	2	3
Si			
$\alpha_i(s)$	1.0	1.5	2.0
$A_i(s)$	1016.0961	-1254.9104	239.1296
$A_{i+3}(s)$	-156.1484	-25.2206	-205.6185
$A_{i+6}(s)$	6.4966	-129.3400	-61.5689
$\alpha_i(p)$	1.0	1.5	2.0
$A_i(p)$	-654.9711	7484.9409	-6829.6058
$A_{i+3}(p)$	90.1852	-1529.2653	-1647.5850
$A_{i+6}(p)$	-3.2880	207.4037	-137.5330
$\alpha_i(d)$	1.0	1.5	2.0
$A_i(d)$	-500.6775	4551.3863	-4050.3467
$A_{i+3}(d)$	70.3747	-906.5957	-938.5709
$A_{i+6}(d)$	-2.6516	138.7125	-70.4548
Si*			
$\alpha_i(s)$	1.0	1.5	2.0
$A_i(s)$	1016.0961	-1254.9104	239.1300
$A_{i+3}(s)$	-156.1484	-25.2206	-205.6185
$A_{i+6}(s)$	6.4966	-129.3400	-61.5689
$\alpha_i(p)$	1.0	1.5	1.0
$A_i(p)$	-654.9711	7484.9409	-6829.6058
$A_{i+3}(p)$	90.1852	-1529.2653	-1647.5850
$A_{i+6}(p)$	-3.2880	207.4037	-137.5330
$\alpha_i(d)$	1.0	1.5	2.0
$A_i(d)$	-500.6775	4551.3863	-4050.3467
$A_{i+3}(d)$	70.3747	-906.5957	-938.5709
$A_{i+6}(d)$	-2.6516	138.7125	-70.4548

so that the potentials are soft core and decay rapidly in momentum space, yet remain accurate. Analytic expressions for the pseudopotentials are determined by fitting to the functional form of Bachelet, Hamann, and Schluter.<sup>14</sup> The pseudopotentials are split into a long-range angular-momentum-independent core potential  $V_{\text{core}}(r)$ , and a short-range angular-momentum-dependent potential  $V_l(r)$  as

$$V_{\text{core}}(r) = (Z_v/r) \sum_{i=1}^2 c_i \text{erf}[(\alpha_i^{\text{core}})^{1/2} r], \quad (3)$$

where  $Z_v$  denotes the valence charge,  $l$  is the angular momentum,  $s$ ,  $p$ ,  $d$ , and  $c_i$ ,  $\alpha_i^{\text{core}}$ ,  $A_i(l)$ ,  $A_{i+3}(l)$ , and  $\alpha_i(l)$  are fitting parameters. The pseudopotentials of Si and Si\* are compared in Fig. 2. The fitted parameters for Si and Si\* are listed in Table II.

The total energy per unit cell of the Si crystal can be written as<sup>15</sup>

$$E_{\text{tot}} = \sum_{n,k}^{\text{occ}} E_{n,k} + \sum_g U(g) + C. \quad (4)$$

The first term is the band-structure energy obtained by summing over occupied bands, the second term involves charge-density-related terms which are written in reciprocal space because of periodicity and includes electron-electron interaction overcounting and exchange-correlation corrections, and  $C$  is an electronic-structure-independent term which includes the nuclear-nuclear repulsion. The exchange correlation used is the parametrized Ceperly-Alder form.<sup>16</sup>

The primitive unit cell of the Si crystal contains two Si atoms and was used to compute the energy-band structure of the ground state. The band structure of the excited state was calculated using a simple cubic large unit cell of eight Si atoms with the one at the origin being replaced by a Si\* atom. The  $spd$  basis set was used in both of the calculations. To ensure that the simple cubic large unit cell is large enough to make the interaction between Si\* atoms small we have also calculated the band structure of the excited state using a large unit cell with 32

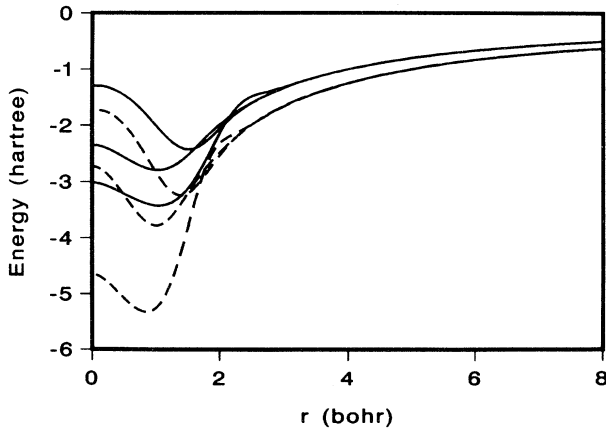


FIG. 2. The  $s$ ,  $p$ , and  $d$  pseudopotentials of Si (solid line) and Si\* (dashed line) from top to bottom.

atoms. Since calculating the density of states using this large unit cell with the  $spd$  basis set is very costly, the minimal  $sp$  basis set was used. The main features calculated using the simple cubic unit cell with eight atoms and the  $spd$  basis set were confirmed by the results calculated using the large unit cell of 32 atoms and the  $sp$  basis set. In calculating the band structure of the excited state there is an electron in the conduction band due to the fact that Si\* has five valence electrons. The effect of this conduction-band electron on the density of states was checked by removing it and leaving a positive charge in each unit cell. The difference between the two calculations is negligible.

### III. ELECTRON-ENERGY-LOSS CROSS SECTION

In the Born approximation the differential cross section for the electronic transition from state  $I$  to  $F$  is given by<sup>17</sup>

$$\frac{d\sigma(\Omega)}{d\Omega} = \frac{4}{a_0^2} \frac{q_f}{q_i} \frac{1}{q^4} \left| \left\langle \Psi_F \left| \sum_j e^{iq \cdot r_j} \right| \Psi_I \right\rangle \right|^2, \quad (5)$$

where  $a_0$  is the Bohr radius,  $\Psi_I$  and  $\Psi_F$  are the many-electron determinantal wave functions of the initial and final states of the target.

For the case of closed-shell initial states, summing over final states and integrating over the Brillouin zone reduces Eq. (5) to Eq. (6) if only single-center integrals are

TABLE II. Pseudopotential parameters of Si and Si\* in atomic units.

$i$	1	2	3
Si			
$c_i^{\text{core}}$	2.27	-1.27	
$\alpha_i^{\text{core}}$	1.08	0.86	
$\alpha_i(s)$	1.38	2.53	3.59
$A_i(s)$	45.8156	-34.4998	-7.2849
$A_{i+3}(s)$	-13.4345	-46.7208	7.6415
$\alpha_i(p)$	1.20	2.97	4.12
$A_i(p)$	1.9619	-27.7211	28.7409
$A_{i+3}(p)$	-0.1096	20.1843	14.9523
$\alpha_i(d)$	2.0	2.70	3.59
$A_i(d)$	2933.0123	-612.7957	-2317.8988
$A_{i+3}(d)$	-654.7819	-2712.7676	-746.0542
Si*			
$c_i^{\text{core}}$	2.27	-1.27	
$\alpha_i^{\text{core}}$	1.44	1.15	
$\alpha_i(s)$	1.13	2.67	3.20
$A_i(s)$	-4.8416	-1532.7349	1543.5194
$A_{i+3}(s)$	0.1623	442.6451	394.2666
$\alpha_i(p)$	1.20	1.67	2.40
$A_i(p)$	129.8759	29.2794	-154.2021
$A_{i+3}(p)$	-15.1765	-110.6051	-46.5303
$\alpha_i(d)$	1.0	1.34	1.73
$A_i(d)$	2748.5951	2048.7603	-4794.3121
$A_{i+3}(d)$	-244.7523	-1818.1740	-744.5422

included and the random-phase approximation is applied:<sup>18</sup>

$$\frac{d^2\sigma(E, \Omega)}{dE d\Omega} = \frac{8}{a_0^2} \frac{q_f}{q_i} \frac{1}{q^4} \sum_j \rho_j(E) |\langle \phi_j | \exp(i\mathbf{q}\cdot\mathbf{r}) | \phi_i \rangle|^2, \quad (6)$$

where  $\phi_i$  and  $\phi_j$  are the core and valence atomic orbitals, and the projected density of states from the  $j$ th valence atomic orbital at energy  $E_f = E + E_i$  is given by

$$\rho_j(E) = \frac{1}{V_{\text{BZ}}} \sum_f \int |C_{j,f}(\mathbf{k})|^2 \delta(E_f - E_i - E) d\mathbf{k}, \quad (7)$$

and  $V_{\text{BZ}}$  is the volume of the Brillouin zone. Our earlier work<sup>19</sup> showed that the random-phase approximation is very accurate and Eq. (6) was used in the present work to calculate the electron-energy-loss cross sections.

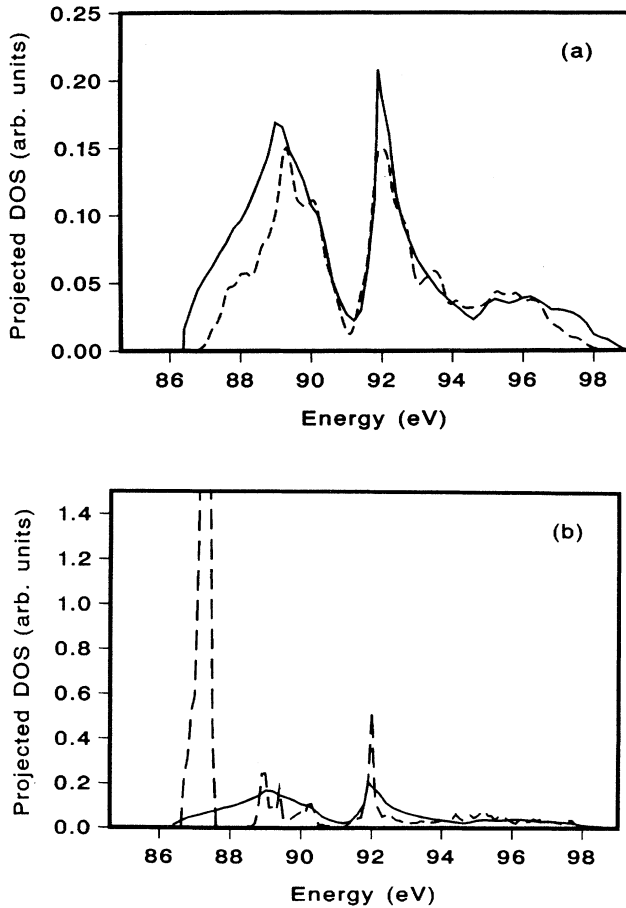


FIG. 3. Comparison of the Si 3s PDOS (dashed line) with experiment (solid line). (a) 3s PDOS calculated from the ground-state configuration, Si; (b) 3s PDOS calculated from the excited-state configuration, Si\*. The experimental data shown in both figures are the same. The vertical scales are different to show the difference in the theoretical results clearly.

#### IV. RESULTS AND DISCUSSION

As discussed in Sec. I, there are two goals in this work. They are the evaluation of the relaxation effect of valence electrons in the x-ray-emission spectra and the excitonic effect of electron-energy-loss near-edge structure of the Si  $L_{2,3}$  edge.

The x-ray-emission spectra of the Si  $L_{2,3}$  edge is due to the electronic transition from the valence band to the  $2p$  core hole. In the dipole approximation only  $3s$  and  $3d$  orbitals can contribute to the total intensity. The calculated projected density of states (PDOS) of the  $3d$  orbital is very small compared to that of the  $3s$  orbital. So only the PDOS of  $3s$  orbital need be considered. The  $3s$  PDOS of the ground-state configuration is compared with the experimental results of Bruhwiler and Schnatterly<sup>20</sup> in Fig. 3(a). The agreement between the theory and experiment is very good. The  $3s$  PDOS of Si\* calculated from the excited-state configuration is compared with the experiment in Fig. 3(b). The  $3s$  PDOS of Si\* has a very large peak on the bottom of the valence band, which does not exist in the experiment. Obviously, the agreement between the  $3s$  PDOS of Si\* and the experiment is not good. The procedure we have used to calculate the energy-band structure of the excited state corresponds to complete relaxation of the valence-band electrons. Our results indicate that there is very little relaxation of the valence electrons before the hole is filled by one of the valence-band electrons.

The calculated electron-energy-loss cross section of the Si  $L_{2,3}$  edge using the ground-state configuration is compared with the experimental results of Batson *et al.*<sup>21</sup> in Fig. 4. The overall agreement is good except that the position of the major peak in the calculated cross section is at a slightly higher energy loss than that of the experiment. The calculated electron-energy-loss spectroscopy (EELS) cross section of the Si  $L_{2,3}$  edge of the excited

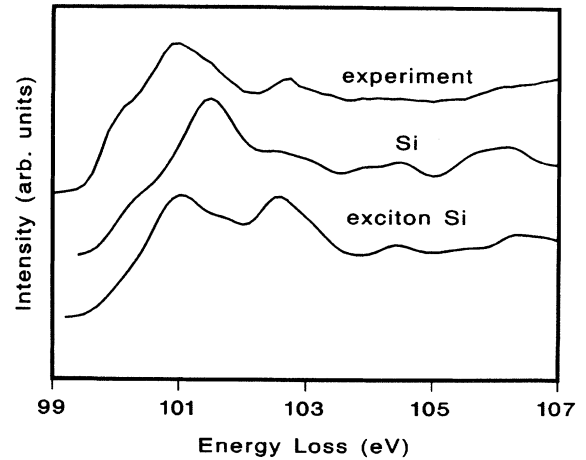


FIG. 4. Comparison of theoretical and experimental Si  $L_{2,3}$  electron-energy-loss near-edge structure. The curve labeled "Si" was calculated using the ground-state configuration. The curve labeled "exciton Si" was calculated using the excited-state configuration, Si\*.

state is also plotted in Fig. 4. The major peak is now at the same position as that of the experiment, but the relative intensity of this peak is lower than that of the experiment.

We have shown that there is very little valence-electron relaxation before the  $2p$  core hole is filled and since the electron-energy-loss process occurs before the x-ray emission we should also expect the valence electrons to stay the same as the ground state. The reduced intensity in the major peak of the lower curve of Fig. 4 could be due to the valence-electron relaxation which was assumed in the band calculation of the excited state. Our results suggest that the right procedure to calculate the Si  $L_{2,3}$  EELNES is to do a ground-state calculation and then perturb only the unoccupied final-state wave functions with the  $2p$  core hole while leaving the valence band unchanged.

## V. CONCLUSIONS

A comparison of our theoretical results with experimental x-ray-emission and electron-energy-loss spectra of the Si  $L_{2,3}$  edge suggests that there is little relaxation of valence-band electrons before the  $2p$  core hole is filled by a valence electron. When including the excitonic effect in EELNES calculations the valence band should be kept the same as the ground state.

## ACKNOWLEDGMENT

This research was supported by Grant No. DE-FG02-87ER45305, U.S. Department of Energy, Basic Energy Sciences, Division of Materials Sciences.

<sup>1</sup>F. C. Brown and O. P. Rustgi, Phys. Rev. Lett. **28**, 497 (1972).

<sup>2</sup>J. P. Van Dyke, Phys. Rev. B **5**, 4206 (1972).

<sup>3</sup>R. S. Knox, *Theory of Excitons* (Academic, New York, 1963), Suppl. 5.

<sup>4</sup>R. J. Elliott, Phys. Rev. **108**, 1384 (1957).

<sup>5</sup>M. Altarelli and D. L. Dexter, Phys. Rev. Lett. **29**, 1100 (1972).

<sup>6</sup>J. Robertson, Phys. Rev. B **28**, 3378 (1983); J. Robertson, *ibid.* **29**, 2135 (1984).

<sup>7</sup>H. P. Hjalmarsen, H. Buttner, and J. D. Dow, Phys. Rev. B **24**, 6010 (1981).

<sup>8</sup>E. J. Mele and J. J. Ritsko, Phys. Rev. Lett. **43**, 68 (1979).

<sup>9</sup>M. M. Disko, J. C. H. Spence, O. F. Sankey, and D. Saldin, Phys. Rev. B **33**, 5642 (1986).

<sup>10</sup>Alex Zunger, Phys. Rev. Lett. **50**, 1215 (1983).

<sup>11</sup>R. W. Jansen and O. F. Sankey, Phys. Rev. B **36**, 6520 (1987).

<sup>12</sup>R. W. Jansen, Dissertation, Arizona State University, 1987.

<sup>13</sup>D. Hamann, M. Schluter, and C. Chiang, Phys. Rev. Lett. **43**,

1494 (1979).

<sup>14</sup>G. B. Bachelet, D. R. Hamann, and M. Schluter, Phys. Rev. B **26**, 4199 (1982).

<sup>15</sup>J. Ihm, A. Zunger, and M. L. Cohen, J. Phys. C **12**, 4409 (1979).

<sup>16</sup>D. M. Ceperly and G. J. Alder, Phys. Rev. Lett. **45**, 566 (1980). The results have been parametrized in J. Perdew and A. Zunger, Phys. Rev. B **23**, 5048 (1981).

<sup>17</sup>M. Inokuti, Rev. Mod. Phys. **43**, 297 (1971).

<sup>18</sup>W. M. Skiff, R. W. Carpenter, and S. H. Lin, J. Appl. Phys. **62**, 2439 (1987).

<sup>19</sup>H. Ma, R. W. Carpenter, S. H. Lin, and O. F. Sankey, J. Appl. Phys. **68**, 288 (1990).

<sup>20</sup>P. A. Bruhwiler and S. E. Schnatterly, Phys. Rev. B **39**, 12 649 (1989).

<sup>21</sup>P. E. Batson, K. L. Kavanagh, C. Y. Wong, and J. M. Woodall, Ultramicroscopy **22**, 89 (1987).